Available online at www.CivileJournal.org

Civil Engineering Journal

Vol. 5, No. 11, November, 2019

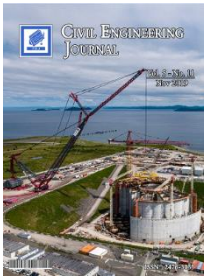

Numerical Study on the Effect of Concrete Grade on the CFT Circular Column's Behavior under Axial Load

Baitollah Badarloo [a*], Faezeh Jafari [b]

[a] Department of Civil Engineering, Qom University of Technology (QUT), Qom 37181-46645, Iran.

[b] Department of Civil Engineering, Malayer University, Malayer 65719-95863, Iran.

Received 26 February 2019; Accepted 03 September 2019

Abstract

Concrete-filled tubular (CFT) column improves the structure properties under different load pattern, so that it should be designed under two main load patterns (static and cyclic load) using current design method such as Finite Element Method (FEM) and analytical method (guideline equation). In this research, a CFT column with specific dimensions is modeled by using ABAQUS finite element software; the target of this study is to conduct a pushover analysis and also a hysteresis analysis under cyclic loading. Then, the concrete grade and percentage of column reinforcement were altered using the FEM, and eventually, compared with the results of analytical equations to measure the safety level of analytical equations. For this purpose, the CFT columns with C20, 30, 40 & 50 concrete cores were modeled with and without reinforcement, and the effect of concrete grade on the capacity of column was studied. In addition, MATLAB software was used to obtain beta index and load capacity design for the CFT column. The results demonstrated that the columns designed in accordance with the AISC have a good performance under the cyclic and static loading. The safety level of design equations ranged between 3 and 5, and the columns could resist higher loads (about 2.5-3.5 times) through the design by ABAQUS.

Keywords: CFT Columns; AISC Guideline; ABAQUS Software; Cyclic and Pushover Analyses.

1. Introduction

The steel sections filled by various grades of concrete with different heights and various compounds are used as column and beam-column in different types of structures. The concrete-filled tubular (CFT) column can improve the structural properties under the earthquake, so that it could develop the same seismic resistance in two perpendicular directions. The composite hollow-section CFT columns show complex stiffness and behavior as a result of the concrete core and the interaction between the two materials. The modulus of elasticity, moment of inertia and effective surface in tensile loading are quite clear in steel, while it is difficult to estimate these parameters in concrete because of heterogeneity. The concrete strength, tensile cracking and prolonged loading effects, among others, have a greater effect on the concrete specifications [1]. Various studies have been conducted to determine the static behavior of CFT columns under axial compressive loads, pure bending, and combined bending and axial compressive loads [2-4], which are outlined as follows. In a numerical study, Ehab Ellobody (2006) examined the behavior and design strength of circular CFT columns under axial loads. This research aimed to investigate the effect of concrete compressive strength ($f'c$) and ratio of diameter to wall thickness (D/t) using the concrete with a compressive strength of 30-110 MPa and the sections with D/t ratio of 15-80. The comparison of the strength obtained from the numerical analysis performed in this study with the design strength calculated using the US, Australian and European codes showed that comparing the European

* Corresponding author: badarloo@qut.ac.ir

http://dx.doi.org/10.28991/cej-2019-03091417

Code, the US and Australian codes provide a more conservative estimate of the CFT column strength [5].

Gupta et al. (2007) conducted an analytical-experimental study on the behavior of CFT columns. This study testing 81 samples examined the effect of diameter to wall thickness ratio of steel section (D/t), ratio of column length to outer wall diameter of section (L/D) and compressive strength of concrete (*f'c*) on the load-bearing capacity of the CFT column. In this research, a nonlinear finite element model was also presented in the ANSYS software environment to study the load-bearing capacity of CFT columns [6]. In a numerical study, Lin-Hai et al. (2008) studied the behavior of the CFT columns under the constant shear and axial loads using the ABAQUS finite element software. According to the results of the study, some relations were presented for the calculation of ultimate strength of the CFT columns under the constant shear and axial loads [7]. Artiomas et al. (2009) examined 1303 samples of CFT column with circular and rectangular sections under the pure axial load and the combined axial and lateral loads. The comparison of the strength from the tests with the corresponding strength obtained from the EC4 regulation showed that the relations of the regulation can correctly estimate the strength, unless the compressive strength of concrete is above 75 KPa [8]. Abedi et al. (2015) studied the effect of creep phenomenon on the CFT columns through the 3D modeling of five series of CFT columns in the ANSYS finite element software. In this research, the effects of parameters such as axial load, concrete age, concrete compressive strength, steel yield strength, and slenderness on the creep behavior of CFT columns were studied by applying the axial load for one year and then, applying the lateral cyclic load. The results of this study showed a moderate 7 and 2% decrease in the ductility and energy loss capacity of the CFT columns as a result of the creep phenomenon, respectively [9].

Raghabendra et al. (2017) numerically studied the seismic behavior of CFT columns used as the bridge piers using Open SEES software. In this study, the effect of parameters such as diameter to thickness ratio, steel grade, concrete grade and slenderness ratio on the lateral bearing capacity of the CFT columns was investigated [10]**.** Using MATLAB to solve reliability and neural network method is current among researchers; the probabilistic method was employed by different researchers such as Lu et al to estimate safety index [11]**.** In some probabilistic and neural network, R^2 is used as the correlation coefficient in the experimental and numerical research [12-14] to obtain the accurate relationship between the experimental and the numerical method [15]. Using the guideline method to estimate the ultimate capacity of concrete structure has been seen in previous research, for example: Jafari et al. (2017) investigated the behavior of concrete beam with the reliability method. The authors used the Monte Carlo simulation to obtain the safety level of ABA guideline [16]. Akbari et al. investigated the safety level for ABA guideline. In this research, the reinforced concrete beam under bending, rectangular sections with the tensile and also compressive rebar, and T-shape sections were designed based on the Monte Carlo method, and the safety index was obtained for the ABA guideline [17]. The present study aims to study the effect of concrete compressive strength and the amount of longitudinal reinforcement on the behavior and the axial compressive and tensile capacity of the CFT columns. It also evaluates the computational relations presented in ASIC to estimate the axial capacity of the CFT columns. For this purpose, a CFT column was modeled in the ABAQUS finite element software for the cases filled with concrete grades C20, C30, C40 and C50 and for different proportions of the longitudinal reinforcement ($\rho = 0$, $\rho = 1.125\%$ and $\rho = 2.250\%$) and subjected to the nonlinear analysis under the cyclic axial load applied on the both tension and compression directions. Then, comparing the analytical results obtained from ABAQUS with the safety values, it was tried to estimate the safety index of composite columns and to study the regulation safety level of the design formulas using the uncertainty method.

2. Materials and Methods

This research investigates the effects grade of concrete on the CFT column's behaviour. Due to do this, the data reported by Soher Guler et al [18] was used for evaluating ABAQUS model. For creating ABAQUS models, tie is used to paste the steel tube to concrete core according to the proposal of composite material; moreover, a nonlinear dynamic analysis and pushover are applied. Finally, the results of FEM analyses were compared with experimental test. In the following, after evaluating ABAQUS model and identifying the concrete grade (C20, C30, C40 & C50), with using some experimental references [18, 19], the relationship between the compressive strength, tensile strength & the Young's modulus was estimated for concrete core. Ultimately, Concrete core for each column was built in ABAQUS and concrete material was assigned to them. Stress-strain curves for compressive and tensile behaviour of concrete (grade 20 to grade 50) were obtained according to experimental reference [19, 20]. Moreover, this model is also able to identify the failure behaviour of the concrete in the ABAQUS [21]. Concrete damage plasticity was used to model a concrete plate. The characteristic of steel was entered into ABAQUS and stress-strain curve was used to show steel plastic behaviour. Steel tube was modelled with using an element type of Shell Homogeneous (S4R) and the bar reinforcement was modelled using the wire element (Beam type) and SOLID element was employed for modelling core concrete. Reinforcement bar is embedded in concrete core. Finally, dynamic analyses test and pushover analyses were employed to evaluated concrete behaviour. After evaluating the CFT column in the ABAQUS software, the MATLAB software was used to assess the guideline equation. To do this, the capacity of each column was obtained by the guideline formulae. The AISC dynamic load was compared with ABAQUS dynamic load in each state (tension and compressive states), and the safety level for AISC equation was obtained by MATLAB software. The flowchart of above process is shown in Figure 1.

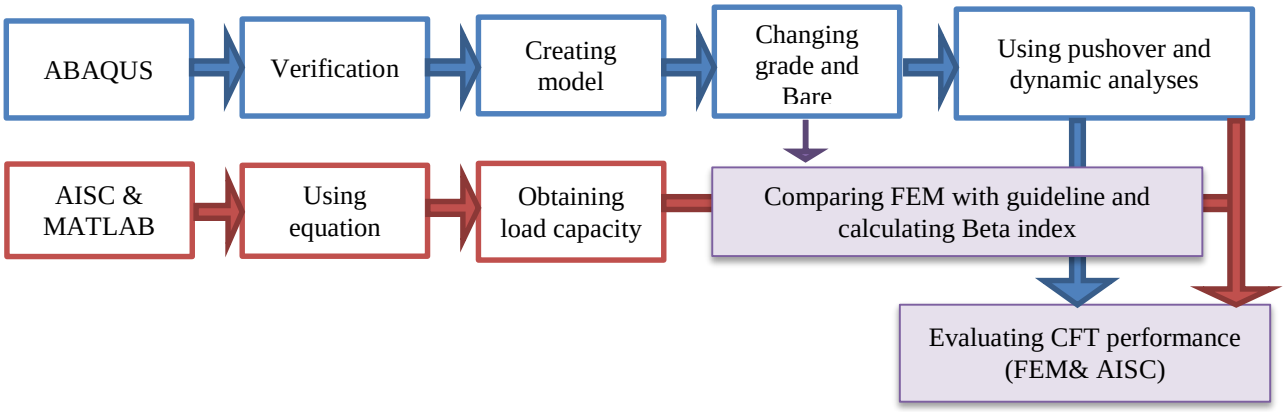

Figure 1. Flowchart of method in present paper

3. Models

In this study, 12 steel samples with the identical circular cross-section filled with concrete of different strength grades were subjected to the reciprocal (dynamic) loads in two cases with and without reinforcement and the results were compared. The material specifications of all modeled samples are presented in Tables 1 and 2, where fc is the compressive strength of concrete, E_c is the elasticity modulus of concrete, E_s is the elasticity modulus of steel, v_c is the Poisson ratio of concrete, and v_s is the Poisson ratio of steel. The unreinforced samples are identified with "CT" and the reinforced samples are identified with "CTB", and the indices are specified based on various concrete strengths. R_t represents the outer radius of the circular tube section, and T_t represents the thickness of steel column, and the specifications are given in Table 2.

Table 1. Parameters calculated in sections

$f_c^{/}$(N/m^2)	E_c (N/m^2)	E_s (N/m^2)	v_c	v_s
2×10^7	2.4×10^{10}	2.1×10^{10}	0.2	0.3
3×10^7	2.80×10^{10}			
4×10^7	3.20×10^{10}			
5×10^7	3.50×10^{10}			

Table 2. General specifications of samples without reinforcement

Load type	Samples			H (m)	d_t (m)	T_t (m)	BARS	
	Group (1)	Group (2)	Group (3)				CT	CTB
Dynamic load	CT20	CTB20,18	CTB20,25	3.1	1.1	0.01	0	10φ18&25
	CT30	CTB30,18	CTB30,25	3.1	1.1	0.01	0	10φ18&25
	CT40	CTB40,18	CTB40,25	3.1	1.1	0.01	0	10φ18&25
	CT50	CTB50,18	CTB50,25	3.1	1.1	0.01	0	10φ18&25

3.1. Specification of Finite Element Model

In this study, ABAQUS 6.14 was used for the modeling of steel CFT columns. The C3D8R (3D 8-node linear isoperimetric element) was used to model the concrete core. This element has the capability of modeling the creep and plastic deformation, and the Four-node shell element (S4 and S4R) was used to model the steel wall. Figure 2 shows the schematic of CFT column.

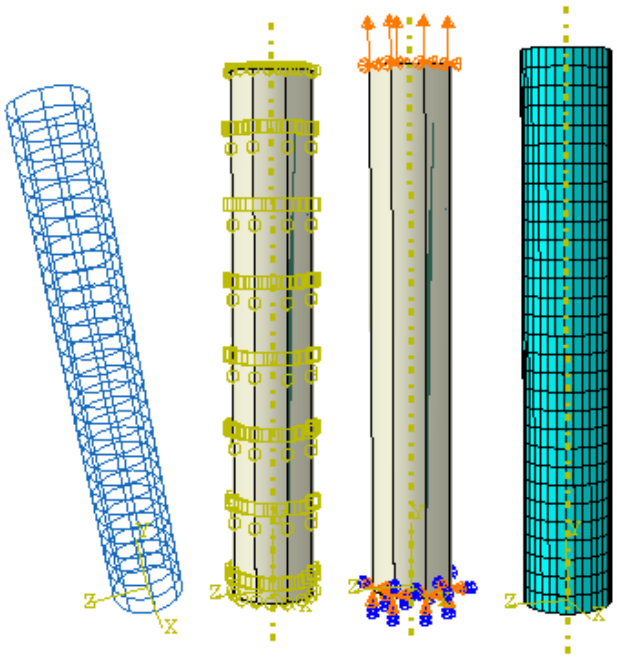

Figure 2. Loading and meshing applied on samples

3.2. Loading and Dynamic Analysis

In this study, the cyclic load pattern shown in Figure 3 is used to study the behavior of CFT columns under the axial cyclic load in accordance with the requirements of ATC-24 (24). The axial load in this study was applied as displacement control, and to uniformly apply loads and prevent the occurrence of stress concentration, a 50 mm steel plate connected to the top end of the column was used.

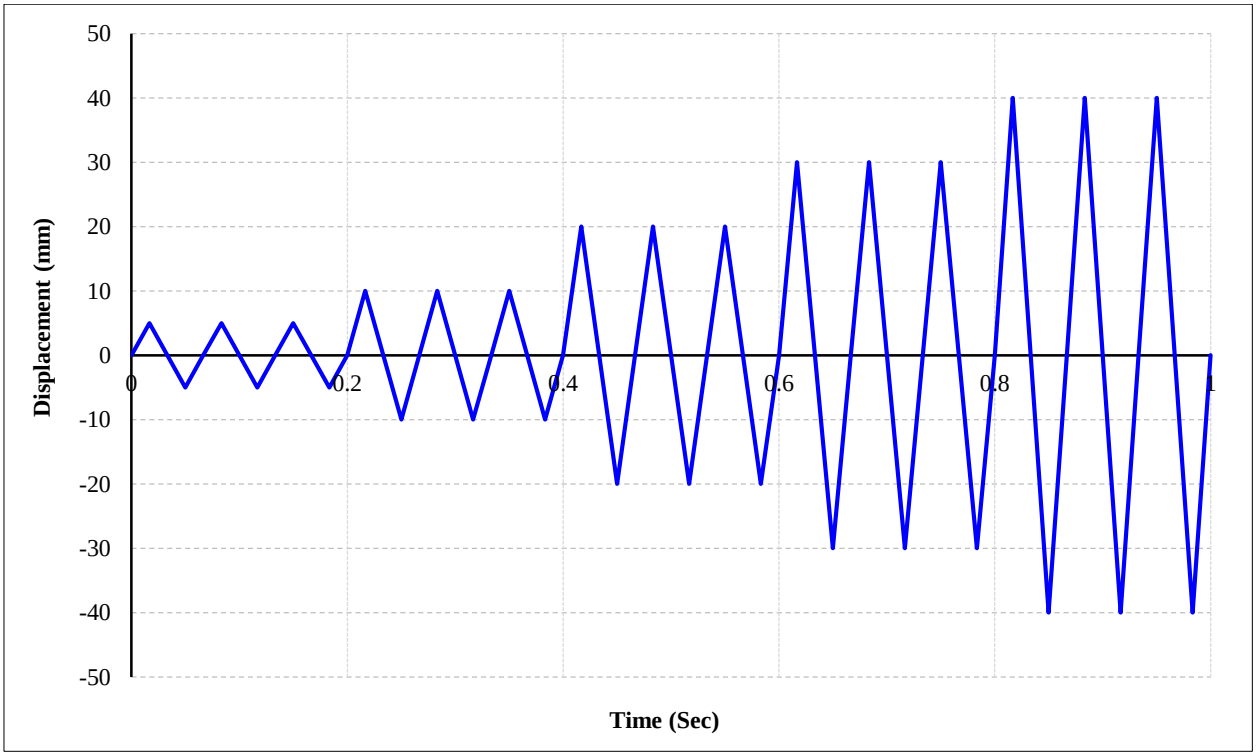

Figure 3. Load curve for samples

3.3. Analysis Type

In the present study, the nonlinear static analysis (pushover) was used for the static loading, and the nonlinear dynamic analysis was used for the cyclic loading.

4. Verification of Modeling

In this part of the study, in order to validate the modeling of CFT column, one of the samples of CFT columns tested by Soher Guler et al [15], it was modeled in the ABAQUS software and subjected to the nonlinear analysis of the axial compressive load. The sample of the CFT column consists of a square CFT column with the height of 400 mm where the compressive strength of concrete and the yield strength of steel cross-section are 115 and 304 MPA, respectively, and the steel section dimension is 100×100×5 mm. After modeling the desired structure, the static nonlinear analysis method was used to analyze the results. Figure 4 shows the finite element model of the cubic column indicating the collapse as a failure mode of pinching at the end of the column, which is in accordance with the experimental results. Figure 5 shows the curve of load-axial displacement of the desired CFT column based on the results of the test and element analysis. As shown in Figure 5, the ultimate axial bearing capacity corresponding to the test and analysis of finite element is 1654 and 1735 KN, respectively, which indicates the high accuracy of the ABAQUS software in the nonlinear analysis of the composite column. Therefore, the matched pattern of failure, as well as the slight difference in the axial bearing capacity corresponding to the test and analysis of finite element indicates the accuracy of the modeling used in this study for modeling the finite element of the CFT columns.

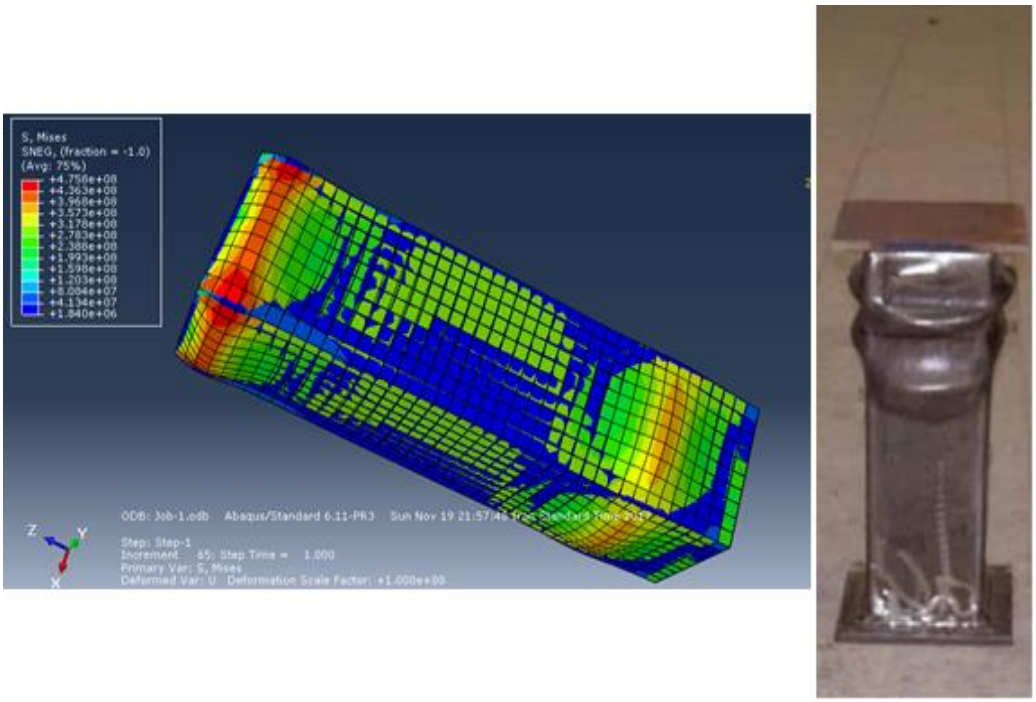

Figure 4. Failure pattern in experimental model and finite element model

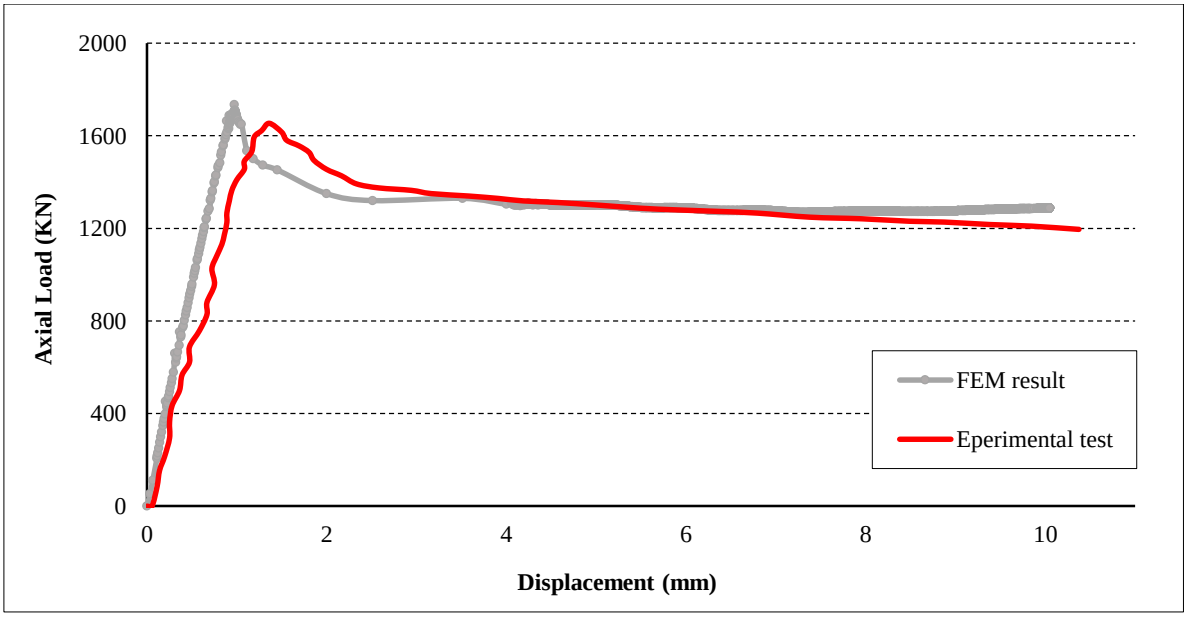

Figure 5. Verification of finite element analysis results

4.1. Cyclic Analysis of Experimental Model

After verifying the present model with the experimental study, the cyclic behavior of a CFT was investigated and compared with the pushover behavior of the present sample. Figure 6 shows that the composite column in the pushover (nonlinear static) analysis exhibits a behavior similar to the nonlinear dynamic (cyclic) analysis in tension and compression. On the other hand, in accordance with the formulas of the regulation, the maximum strength resisted by the column in tension is 333 and in compression is 459, while the results from ABAQUS indicate that this value is 440 and 695 tons, respectively. Comparison of columns in different analyses, as well as comparison of structure responses with the regulation formulas shows that the applied load in cyclical mode is close to the experimental behavior of the column and the regulation formulas in compression calculate lower result. As was shown in the previous section, the pushover results of ABAQUS are close to the experimental results, this section also showed that the stiffness of structure is equal in both cyclic and pushover conditions.

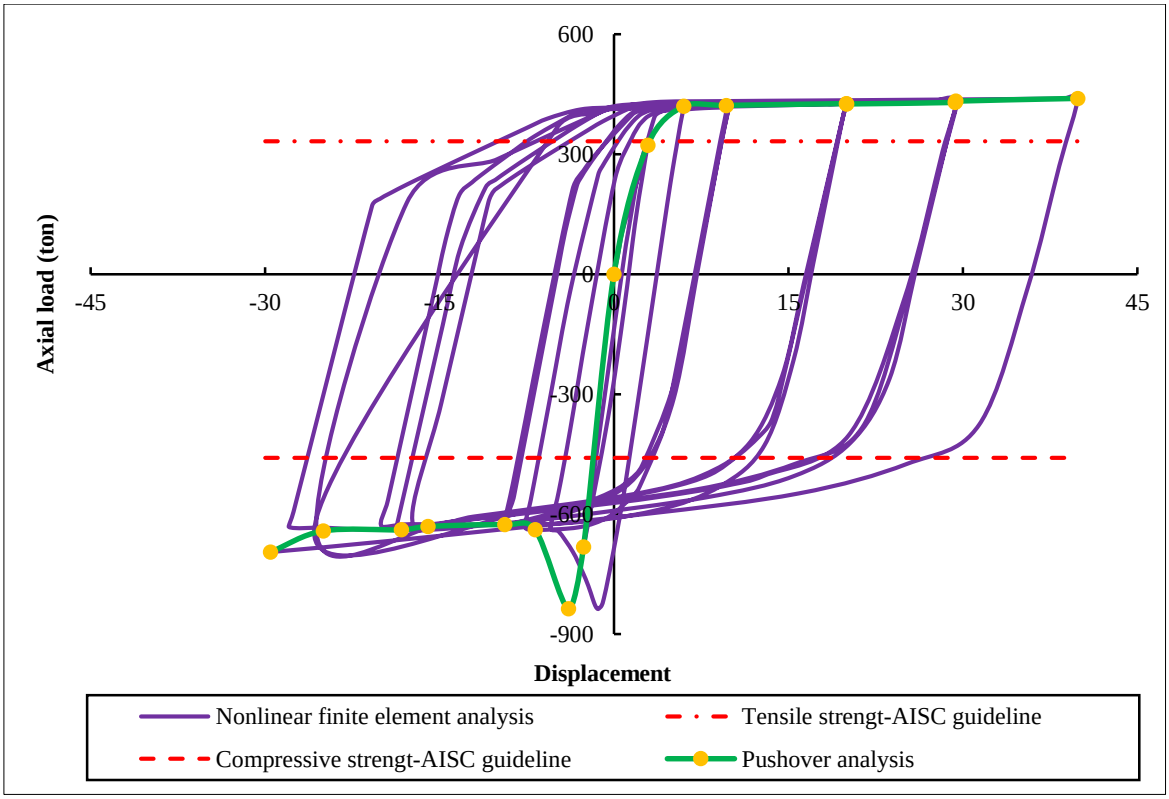

Figure 6. Verification of finite element analysis results

After ensuring the modeling of composite column in ABAQUS software and examining the behavior in both cyclic and pushover conditions, the results obtained from the software are presented.

5. Presentation of Results

5.1. Without Reinforcement

The samples mentioned in the previous section were analyzed using the simulation in ABAQUS software under axial reciprocal (dynamic) loads. The curves obtained from the software analysis are shown in Figures 7-10 for each element of the steel section and concrete core in each sample. As shown in the curves, the tensile region of concrete with different strengths does not have a significant effect on the final performance, and the performance of the CFT column in tension depends on the performance of the steel section. However, in the compressive region of the steel section and concrete core, both of them contribute to the resistance of applied axial load, and with the increase in the strength of concrete core, the contribution of the core to the resistance of the load is considerably increased.

Figure 7 shows the hysteresis diagram for the steel segment of composite column. The behavior of steel section in the tensile and compressive regions is close to each other, and the diagram is symmetric for all composite columns. The increase in concrete grade led to the higher load resistance of steel confinement in the tensile region relative to the other grades. By increasing the concrete grade, it is expected that the column will exhibit a higher stiffness under cyclic loading, and as a result, the steel confinement is required to use its maximum capacity to resist the applied load. Thus, with the increase in the concrete grade, the area of the hysteresis loop and energy absorption is increased, as shown in

Figure 7. The horizontal axis also shows that the increase in the column grade led to a higher ductility in the C30, C40 and C50 grades than in the C20 grade, which is shown in Figure 7 with the arrow.

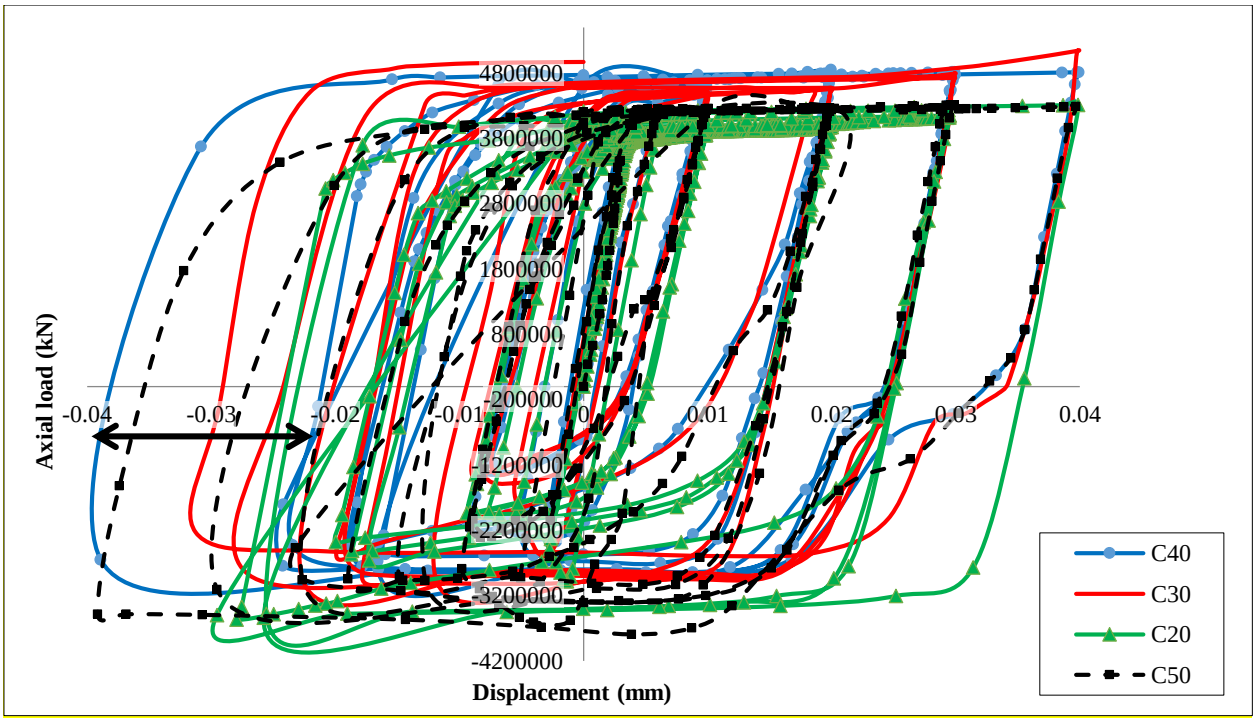

Figure 7. Hysteresis curve of samples without reinforcement for steel confinement

Figure 8 shows the behavior of concrete core in the composite column. As expected, an increase in concrete grade leads to a better behavior of the column in tension and compression in the concrete column. The concrete core along with the steel confinement under the cyclic load applied for all grades tries to use their maximum capacity to resist the load. The behavior of concrete core in tension in all grades is somewhat close together, but these columns have a different behavior. As expected, the major area of the composite column is consisted of the concrete core, and the thickness of steel confinement is 1/10 concrete core thickness. In addition, the behavior of the composite column in tension is mostly affected by the steel confinement and reinforcement. Therefore, it is expected that increasing the concrete grade will not have a significant effect on the behavior of the column in tension. This increase caused that the column in compression utilizes its maximum capacity against the applied loads, and the area of the hysteresis loop is significantly increased in this case.

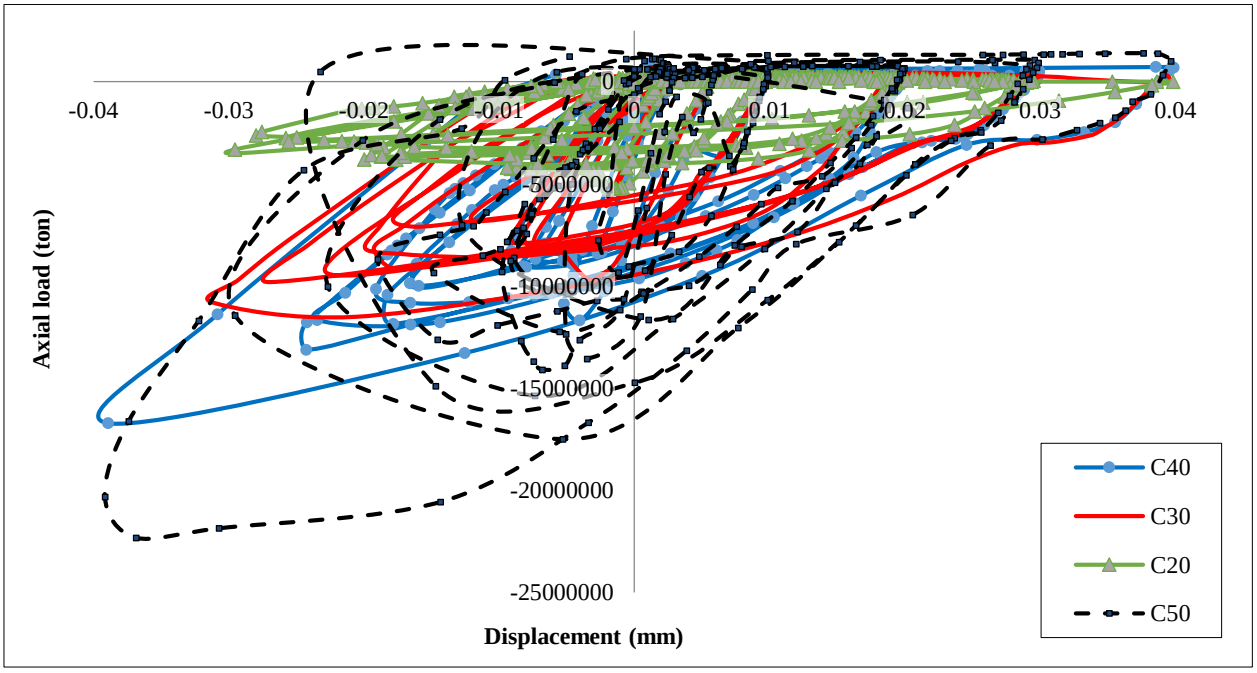

Figure 8. Hysteresis curve of samples without reinforcement for concrete core

Figure 9 shows the behavior of the composite column under cyclic loading. As it is expected, due to the fact that the concrete core forms the major part of the column, the behavior of hysteresis loop in the composite column is mostly affected by the concrete grade. Also, using the concrete grade C50 caused more axial displacement in the concrete column than the C30 grade. Figure 9, on the other hand, shows that the use of steel confinement led to more regular hysteresis loops of the composite column than the concrete core alone. Therefore, the simultaneous use of steel confinement and concrete core helps the hysteresis loop become regular. On the other hand, the behavior of the column in tension is improved, as the load absorbed in the composite column is more than that in the concrete core, and the area of the loop is increased in the tensile region. As shown in Figure 9, if the C20 grade is used in the construction of a composite column, the use of confinement will cause the hysteresis loop to behave in the same manner in both the tension and the compression, and in fact, the behavior of concrete in tension is improved. At higher grades, such as C50, the use of steel confinement led to more regular loops of column than the concrete core. Also, the axial displacement of the column is increased when the column is in compression, so that in the C50 grade, the column could be displaced 1.33 times the C20.

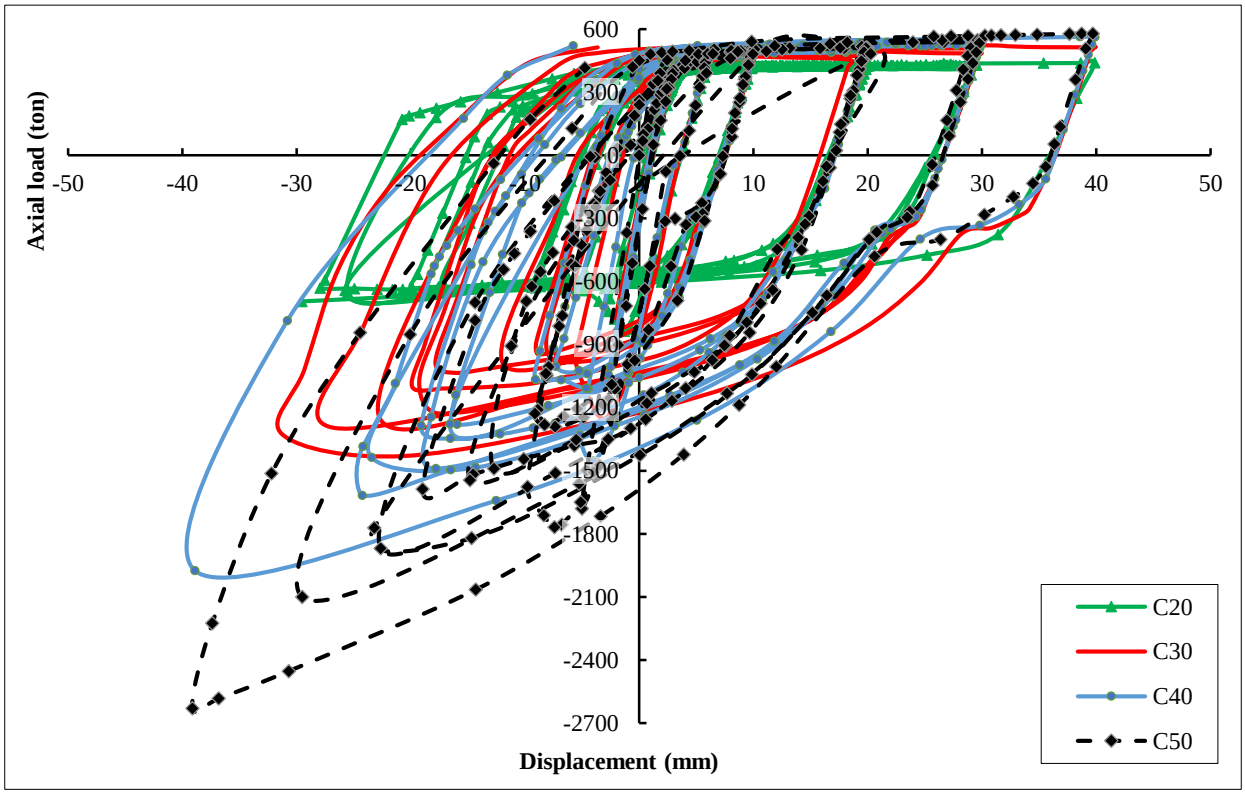

Figure 9. Hysteresis curve of samples without reinforcement for composite column

In the following (Figures 10 and 11), the output results are compared for the composite concrete column in two cases: without reinforcement for CT20 and CT50.

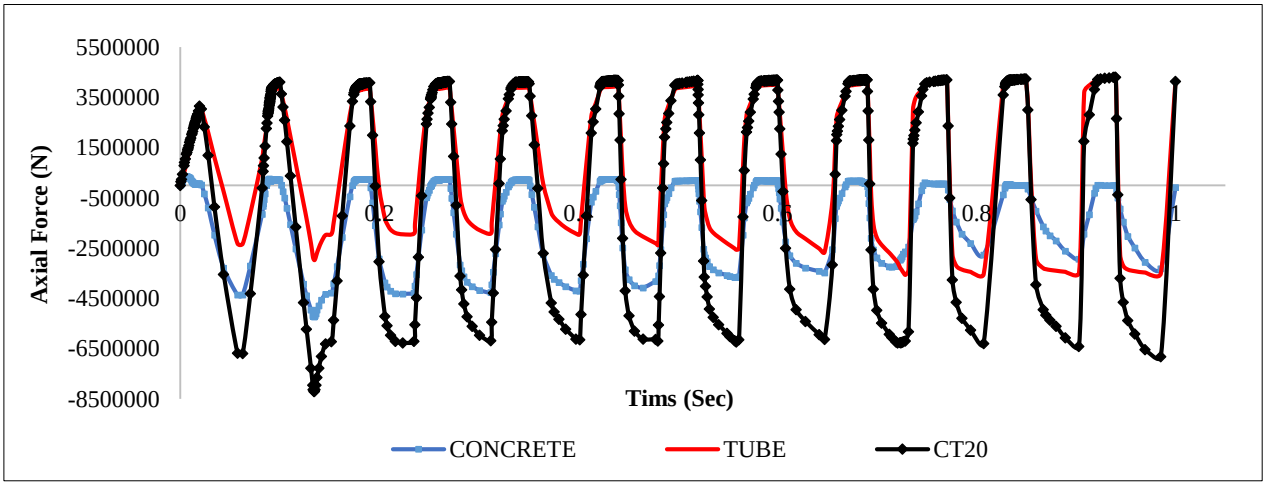

Figure 10. Hysteresis curve of samples without reinforcement for composite column-CT20

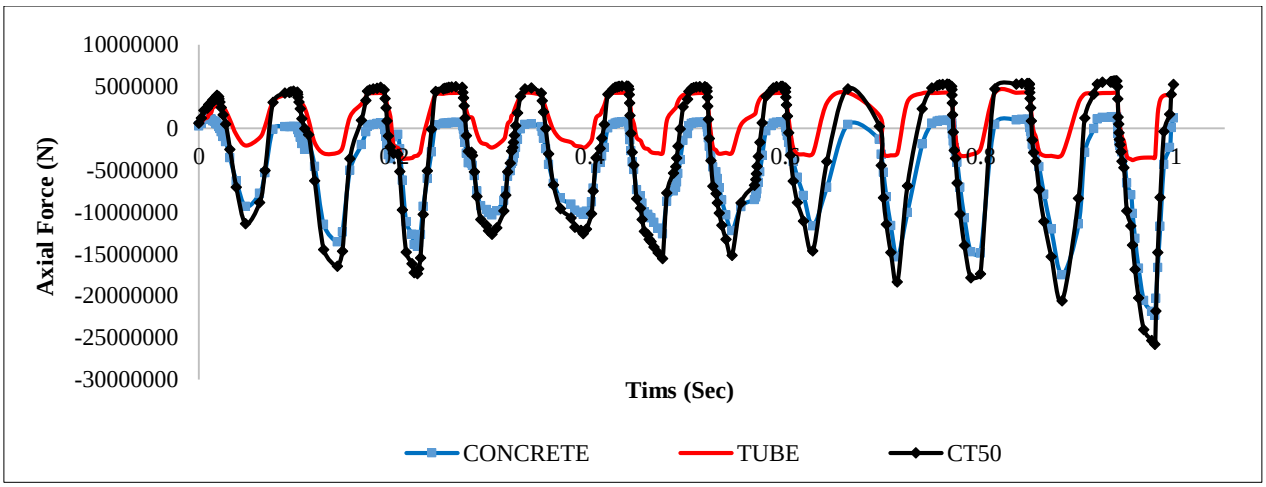

Figure 11. Hysteresis curve of samples without reinforcement for composite column-CT50

5.2. Comparison of Hysteresis Curves of Samples in Case of Using Reinforcement

The hysteresis diagrams of the CT and CTB 18 & 25 samples are shown in Figures 12 and 15, and for a closer examination of the samples, only the load-displacement curve is shown in the figures. The tensile region of steel has the highest contribution to the load resistance, and in the compressive region, concrete resists the major part of the applied load. The combination of concrete and steel creates a composite material that has an acceptable strength in tension and compression. As shown in Figures 12 to 15, increasing the compressive strength of concrete in the tensile region does not have a significant effect on the performance of the samples, but with increasing the compressive strength of concrete in the compressive region, the ultimate strength of the samples is significantly increased. Also, comparing the curves with and without reinforcement, it can be found that the difference in hysteresis curves can be reduced by increasing the compressive strength of concrete. The reinforcement in the composite column is used when the lower grades of concrete are used in the construction of the column.

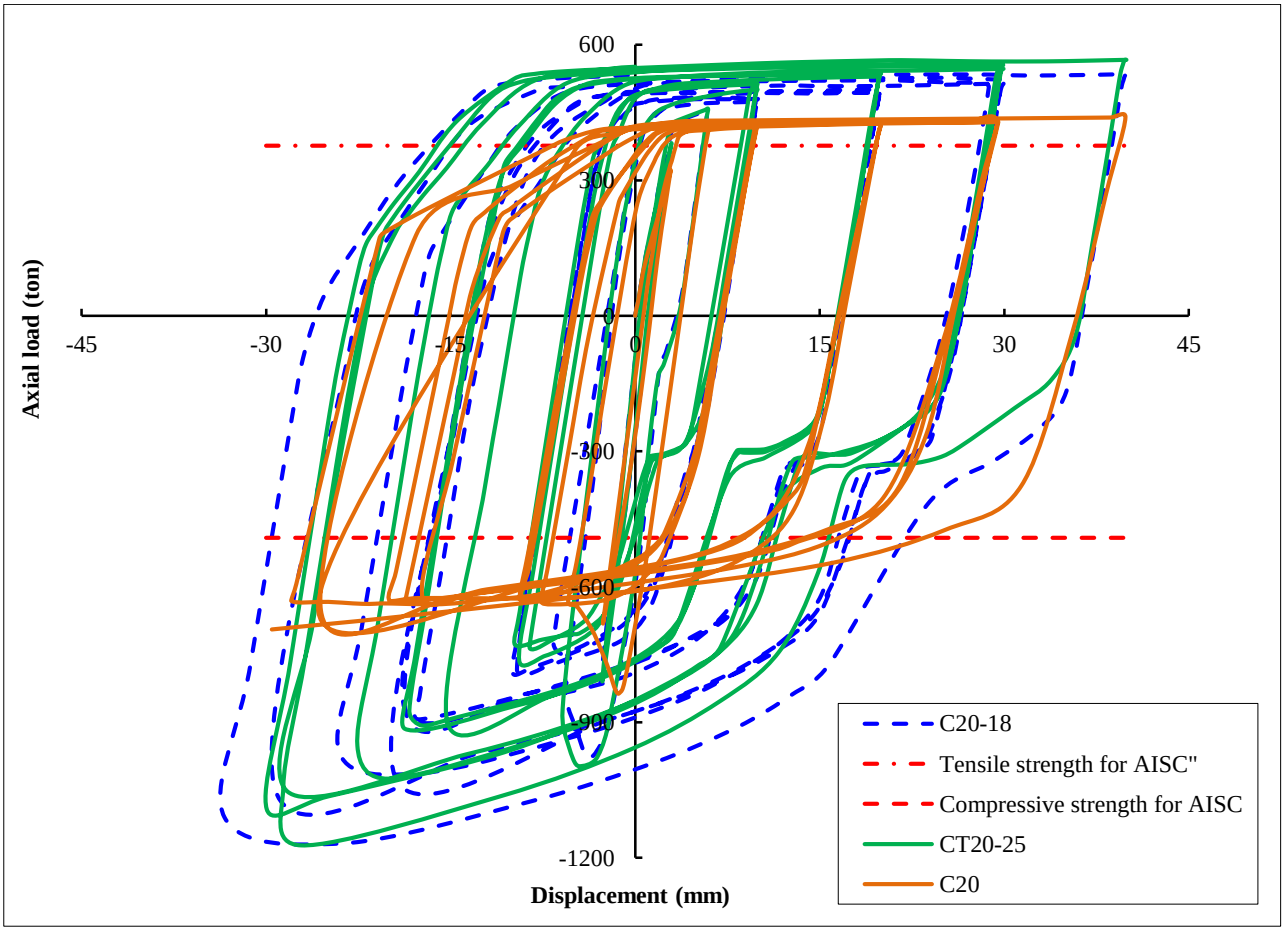

Figure 12. Hysteresis curve for CT20, CTB20-18 and CTB20-25 samples for steel part

The equal amount of steel is used in the all designed models. The main objective is to study the strength of the concrete. Figures 13 and 15 show the load-displacement diagram for each model under simultaneous reciprocal loading. The purpose of simultaneously plotting the diagrams is to observe the difference in the values of the resisted load. The concrete quality was increased 2.5 times in the samples CT20 to CT50, but the loads resisted by the samples, as shown in Figures 13 to 15, indicate an increase of about 5 times, representing the remarkable performance of the samples CT50 and CTB50 under strong axial compressive load. Therefore, it can be predicted that using these sections can be useful in the places that are under the strong axial loads.

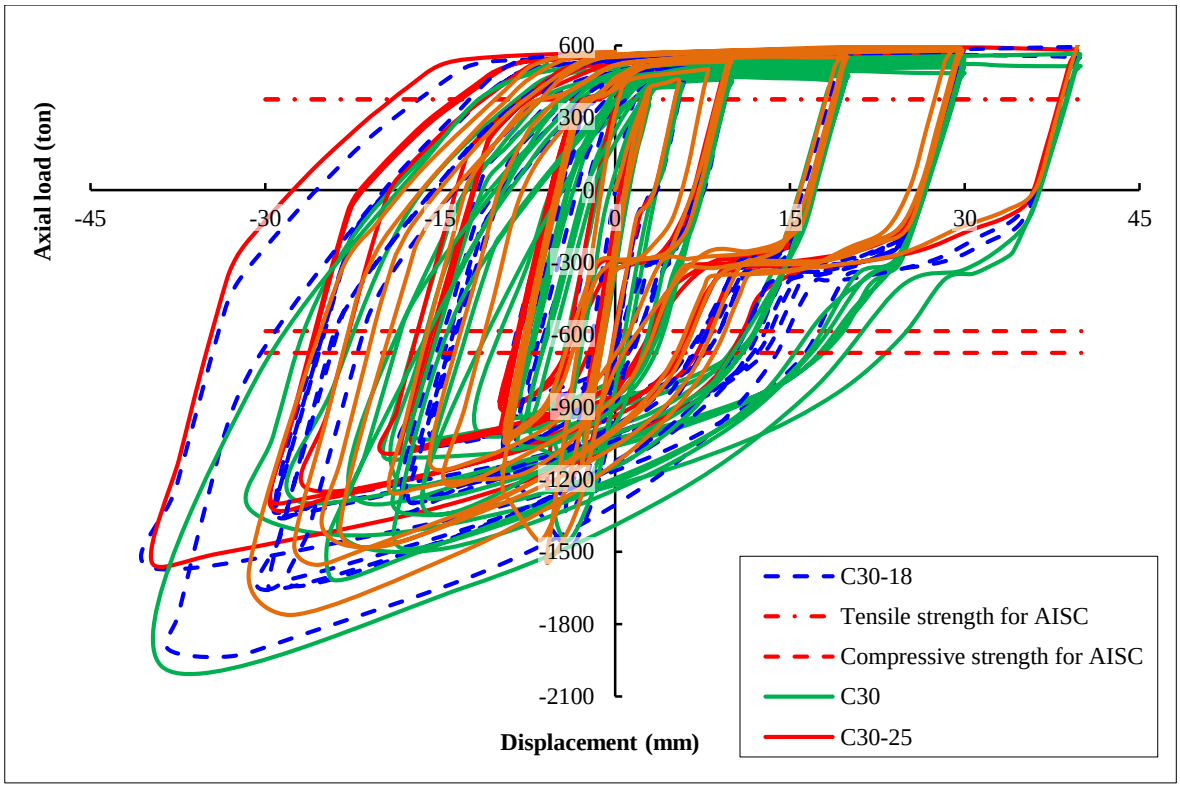

Figure 13. Hysteresis curve for CT30, CTB30-18 and CTB30-25 samples for concrete part

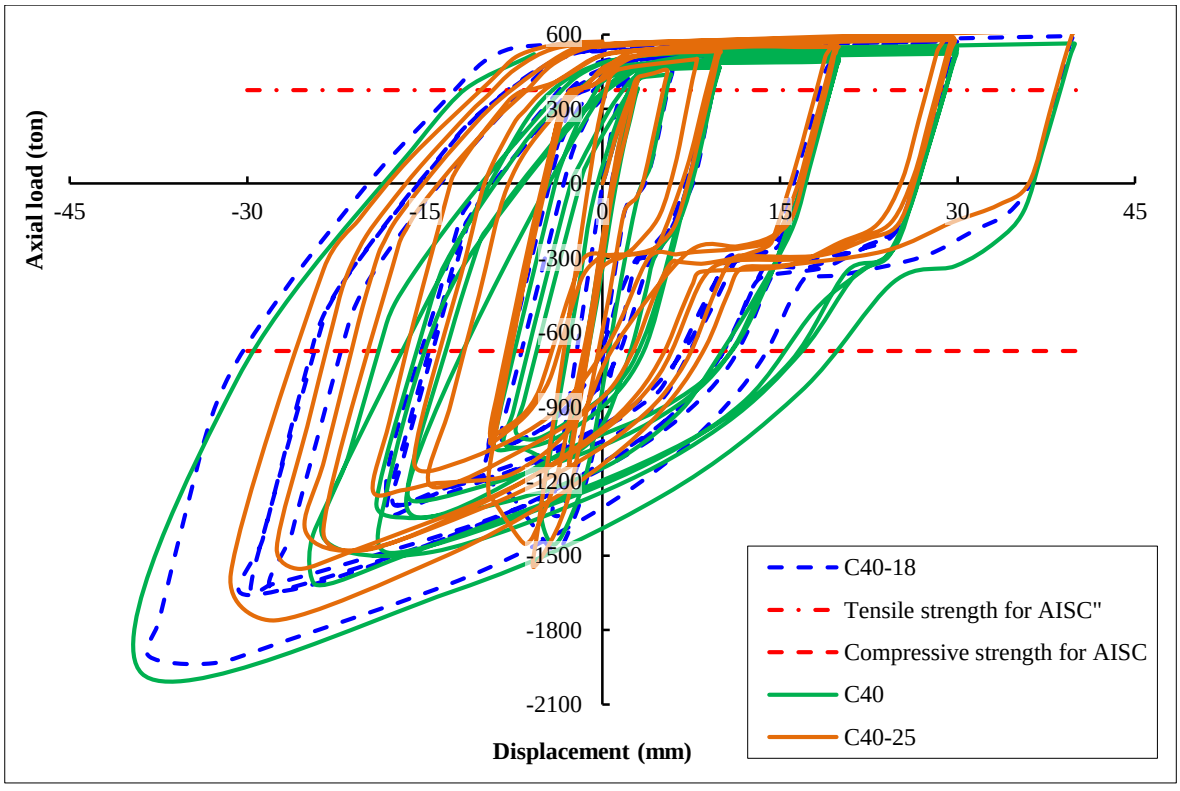

Figure 14. Hysteresis curve for CT40, CTB30-18 and CTB40-25 samples for composite part

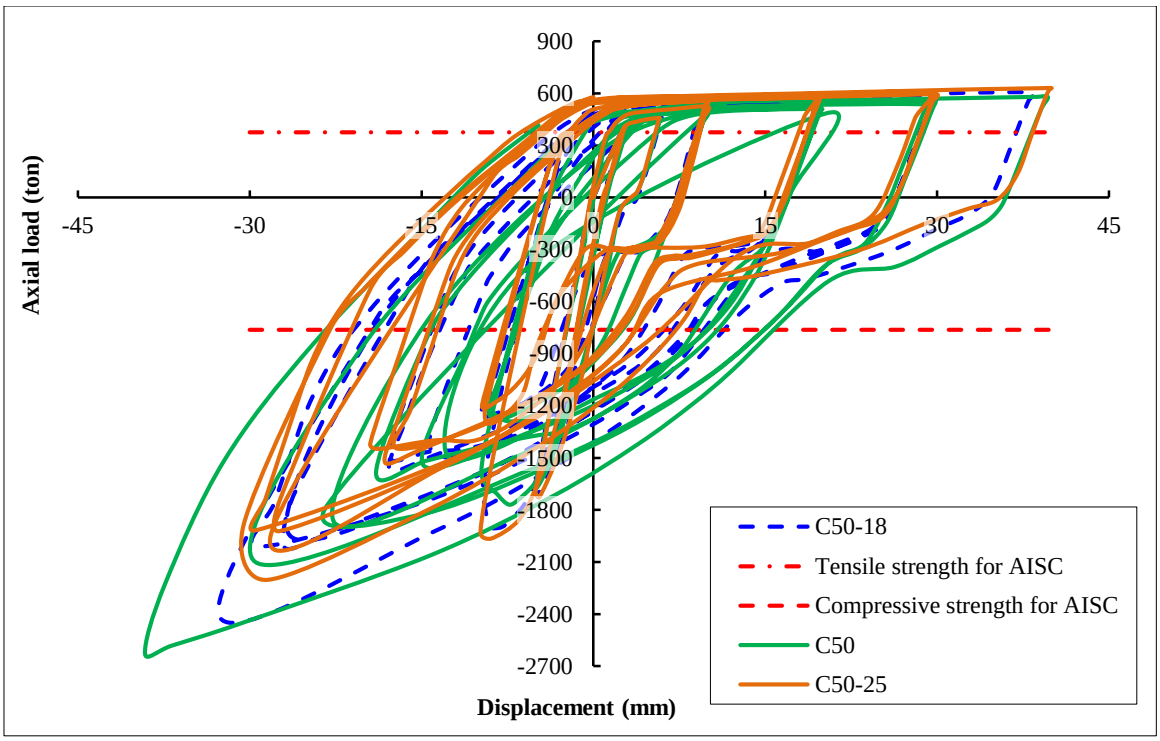

Figure 15. Hysteresis curve for CT40, CTB30-18 and CTB50-25 samples for composite part

As seen from the hysteresis curves of Figures 12 to 15, in CT and CTB samples with lower concrete strength, a uniform behavior in both tensile and compressive regions is seen. The curves are denser, more regular and uniform, but as the compressive strength of concrete is increased, the hysteresis curves in the compressive region become very irregular. However, there is no significant change in the tensile region, and it is evident that the tensile capacity of the CT and CTB samples is entirely dependent on the steel section.

5.3. Pushover Analyses

In the design of the CFT columns, a steel section can be considered proportional to the tensile load, but in compression, the effect of both sections is involved. Due to the confinement effect of the steel section and the prevention of concrete cracking even after the initial cracks and crushing, these types of columns can be used in areas subjected to strong compressive loads. This can be seen as shown in Figures 16 and 17 by plotting the pushover curve.

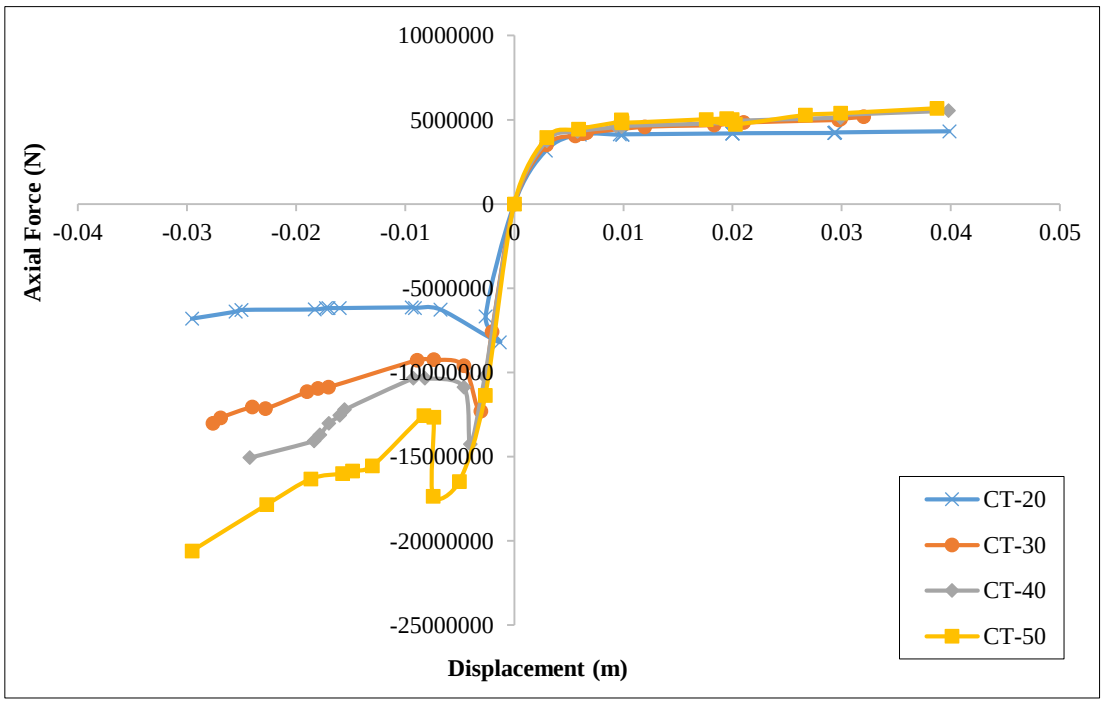

Figure 16. Comparison pushover curve of CT columns

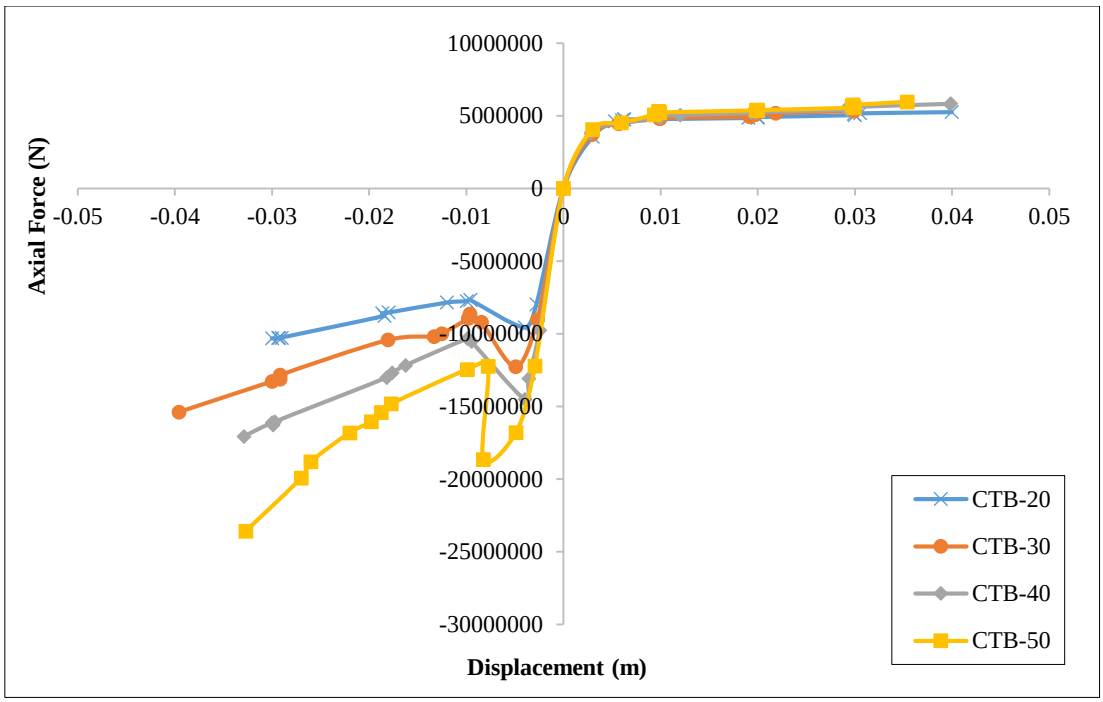

Figure 17. Comparison of pushover curves of CFT columns

Figure 18 presents the stress and displacement of composite column in the CFT column; the increased concrete grade reduces the stress in the CFT layer. The both columns may show acceptable flexibility. The maximum displacement is observed at the top of the column. However, the stress in the column of grade C30 concrete is less than that in the column of grade C50 concrete, because the concrete core employs its maximum capability to absorb the stress, and the better performance causes a decrease in the stress of steel layer.

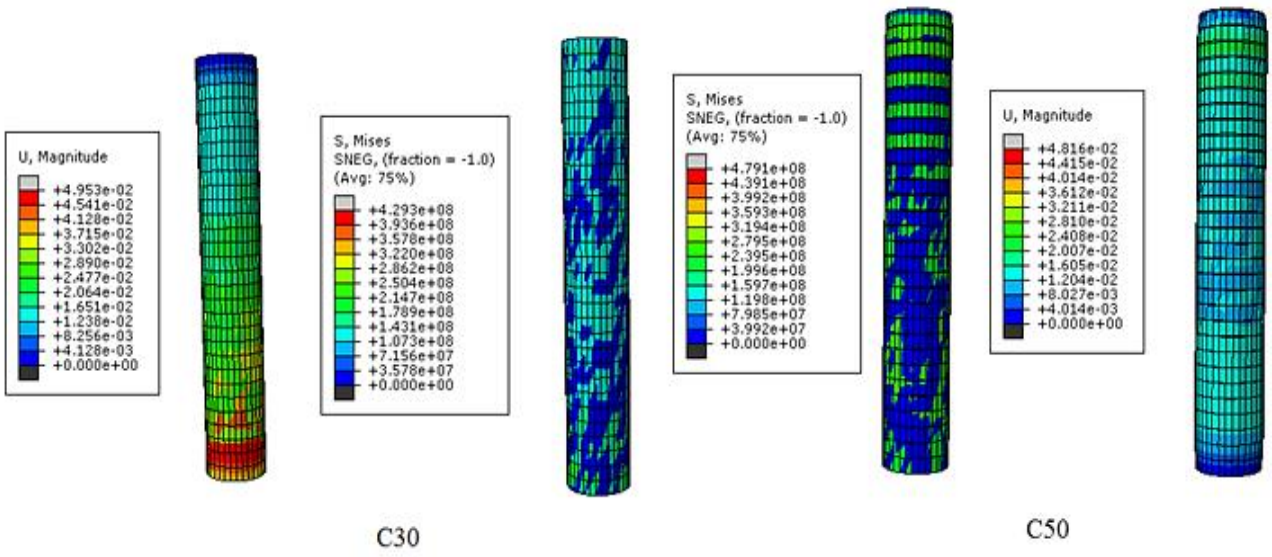

Figure 18. Stress and displacement for C20 and C50 column

6. AISC Relations

In the tenth chapter of the national building regulation, the design compressive strength of axial members with concrete-filled sections in the analyzed CFT columns is obtained according to Equation 1 [1]:

$$P_{no} = F_y A_s + C_2 \left(A_c + A_{sr} \frac{E_s}{E_c}\right) f_c \quad (1)$$

In this equation, C_2 is 0.95 for the circular steel hollow sections. The design tensile strength of the axial members with the concrete-filled section is obtained according to Equation 2:

$$P_t = \emptyset_t \left(A_s f_y + A_{sr} F_{ysr}\right) \quad (2)$$

In this equation, $\emptyset_t$ is 0.90 for the circular steel hollow sections. By calculating the relations in the tenth chapter of the regulation and extracting the corresponding curves, the values presented in Table 4 are obtained. Tables 5 shows the comparison between the maximum values of the analytical results obtained with the ABAQUS software and the corresponding values calculated in accordance with the AISC.

Table 4. Comparison of analytical values with relations from regulation

Compressive State						
Variable	**CT-20**			**CT-30**		
	φ0	**φ18**	**φ25**	**φ0**	**φ18**	**φ25**
Dis. (mm)	29.53	33.38	29.96	31.25	39.58	39.72
Abacus load (kg)	836.67	1168	1172	1430	1568	1545
AISC load (kg)	459	491	521	535	585	614
AISC/Abacus	1.82	2.37	2.24	2.67	2.68	2.51
Tensile state						
Dis. (mm)	39.86	39.96	39.94	39.94	39.94	39.63
Abacus load (kg)	440	535	567	527	562	591
AISC load (kg)	333	376	417	333	376	417
AISC/Abacus	1.32	1.42	1.35	1.58	1.49	1.41
Compressive State						
Variable	**CT-40**			**CT-50**		
	φ0	**φ18**	**φ25**	**Φ0**	**φ18**	**Φ25**
Dis. (mm)	39.90	38.29	31.4	39.14	32.70	30.55
Abacus load (kg)	1974	1993	1761	2630	2405	2202
AISC load (kg)	644	675	704	731	762	791
AISC/Abacus	3.06	2.95	2.50	3.59	3.15	2.78
Tensile state						
Dis. (m)	38.90	39.84	39.87	39.68	38.41	39.99
Abacus load (kg)	564	593	616	579	606	631
AISC load (kg)	333	376	417	333	376	417
AISC/Abacus	1.69	1.57	1.47	1.73	1.62	1.51

The results of the table (Table 4) indicate that steel reinforcement causes an increase in the tensile and compressive capacity of column in the C20 and C30 grades of concrete. In higher grades of concrete, however, the increased reinforcement enhances the tensile capacity of section rather than compressive capacity; while the code equations for all grades of concrete recommend that the addition of reinforcement increases in the compressive capacity of column in whole grades of concrete. On the other hand, the AISC guideline estimates the compressive and tensile capacity of column in the C20 and C30 grades closer to the finite element values, but the increased grade of concrete causes the AISC to estimate the values more conservatively. The addition of reinforcement to the concrete also makes the AISC values closer to FEM result, particularly in the C40 and C50 grades. In lower grades, the addition of steel reinforcement to the column increases the column displacement (column flexibility) within its compression region. In higher grades, however, the increased flexibility is more limited in the tensile region and the capacity of column rises in that region; therefore, it can be argued that the AISC formulas cannot estimate the column capacity within a constant range for entire grades of concrete.

6.1. Safety Level of Column Designed with Regulation Relations

More precise results of design parameters such as dimension, compressive strength, etc. indicate that the considered problem, e.g. compressive strength of concrete, requires more detailed parameters, each of which has uncertainty. Therefore, a specific random nature can be considered for each of the partial parameters. After determining the random nature of the parameters, the behavior of composite columns is addressed considering the uncertainty factors. In this method, the failure function and the load and strength equations are determined and specific statistical data and distribution are also found. Then, the obtained values are replaced in the equations. The values of the strength function will be the same as those found in the lab on a real sample. The advantage of this method is that it will be much easier to replicate and generate the sample on the computer, and we will be able to do the simulation at a lower cost several times, (perhaps 10,000 times), and then, perform the statistical work on the results. For example, the standard deviation

and average of the data will be able to be calculated, and by substitution in Equation 3, the safety index could be calculated [16, 17], using safety index (beta) equation. Equation 3 shows the value of (β), in this equation, μ_{RPn} is resistance capacity which is obtained with Equation 3 and μ_{SPn} is axial load and σ^2_{RPn} and σ^2_{SPn} are the variance of resistance capacity and axial load, respectively.

$$\beta = \frac{\mu_{RPn} - \mu_{SPn}}{\sqrt{\sigma^2_{RPn} + \sigma^2_{SPn}}} \quad (3)$$

In the surrounding phenomena, there are parameters that do not have a definite value and show a random nature. Extensive efforts have been made for the formulation of engineering regulation in order to secure structures and to identify uncertainties in the design parameters. Safe design requires that the load applied on the structure does not exceed the strength. However, the required difference depends on the distribution of design parameters around the average. Therefore, it is necessary to make a series of statistical studies on the design parameters before expressing each parameter in order to determine the uncertainty associated with each statistical parameter. The following table (Table 5) shows the parameters containing the uncertainty used in the research.

Table 5. Table of nominal values used in problem [16, 17]

Design specifications				
Cross section	**Index**	**mean**	**St**	**Distribution fit**
Steel area	A_s	A_s	$0.03 * A_s$	Normal
Compressive strength	f_c	f_c	$0.0093 * f_c$	Normal
Tensile strength	f_y	f_y	0.01	Normal
Dead load	q_D	$1.05 * q_D$	$0.1 * q_D$	Normal
Live load	q_L	q_L	0.3	Gamble
Concrete area	A_c	A_c	$0.03 * A_c$	Normal
Modulus of elasticity	E	E	0.1	Normal

Considering the above table and using the Monte Carlo method, the coefficient of strength in design is 0.75 and the dead and live load coefficients are 1.2 and 1.6 in accordance with the AISC, respectively. The safety index of the designed column is further calculated for the 12 columns designed in the study and summarized in Figure 19. Also, the safety index for the strength value obtained in ABAQUS is presented in Figure 19. If we reduce the $+C_2$ coefficient, the strength value obtained by the regulation relations becomes close to the values from ABAQUS, while the probability of structure failure is increased in accordance with the regulations, and also the safety index is increased. Equation 3 shows how to obtain the safety index, and Equation 4 also shows the failure probability of the composite column. The method for achieving the safety level and the failure probability of design equations is based on the research, and the safety level of 3-3.5 is reported in the AISC. Figure 19 shows the relationship between P_n and Beta) with sample and without armature.

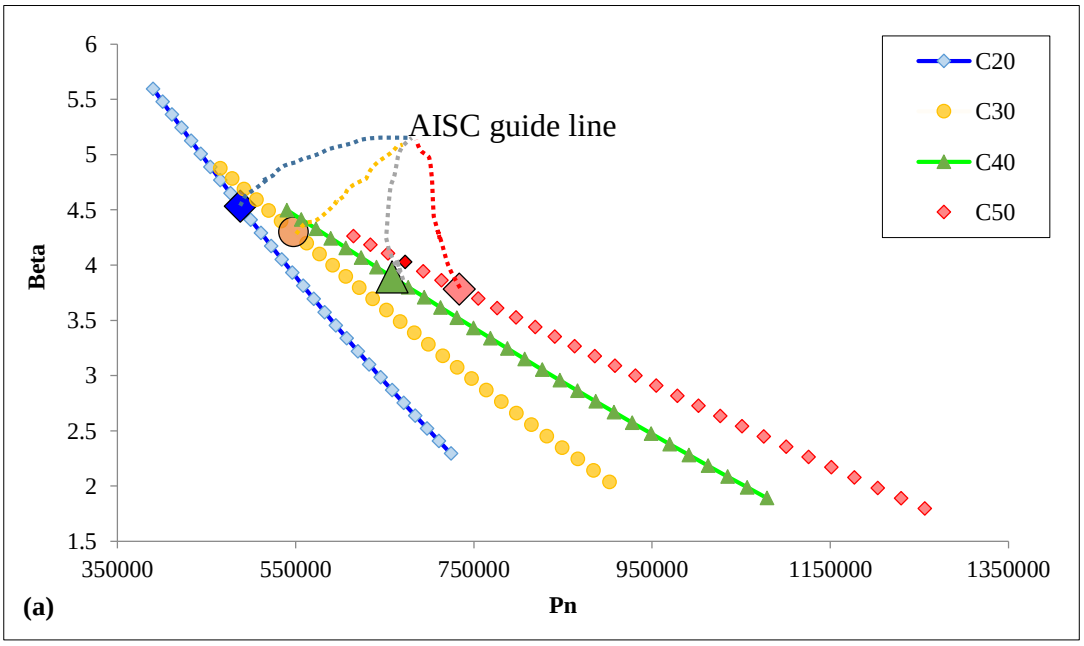

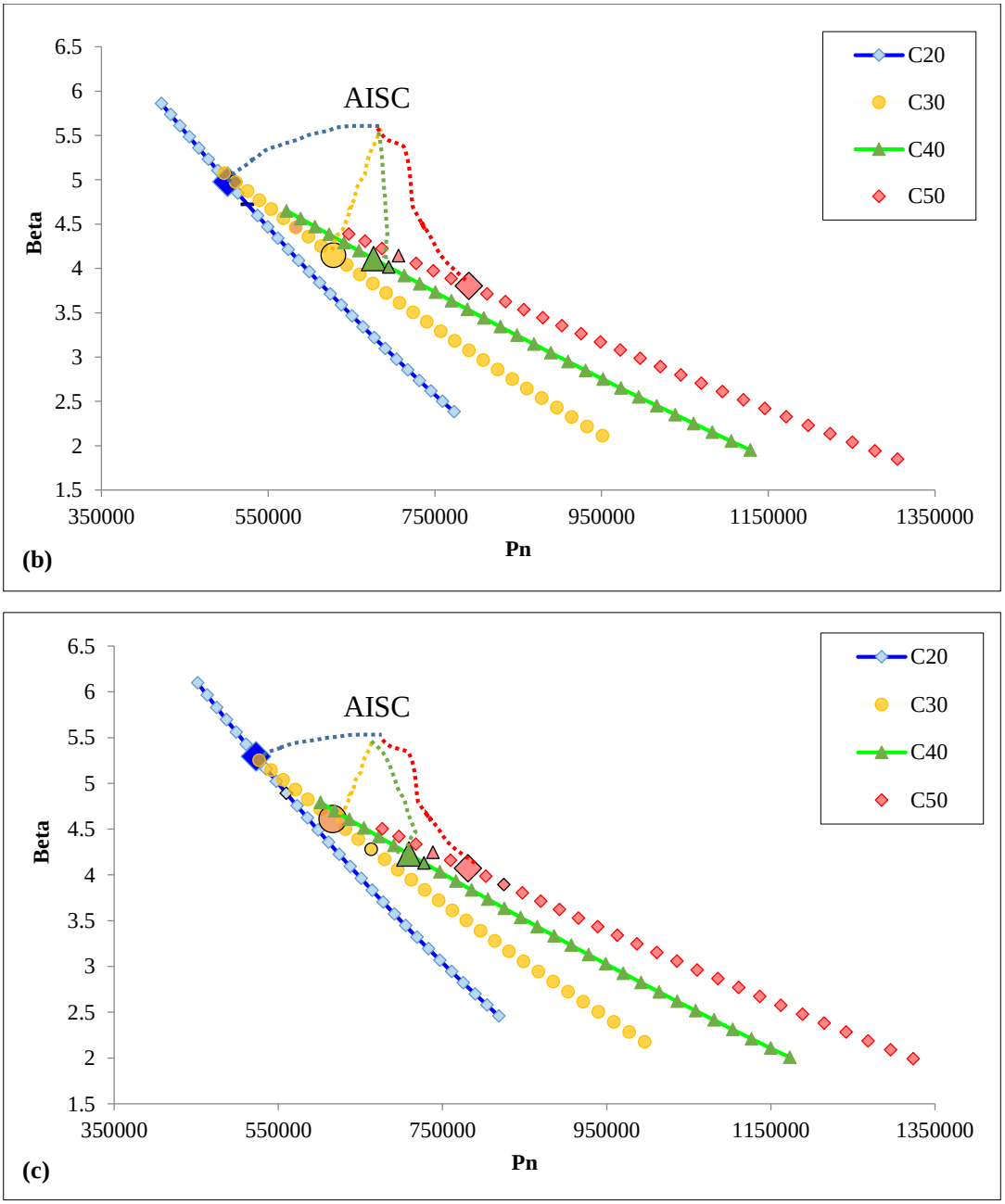

Figure 19. The relationship between Beat and Pn

The trend of graphs shows that the use of steel reinforcement and increase in its diameter result in an increase in the safety factor due to the addition of steel in the concrete section; because the strength reduction factor ($\emptyset_s$) versus the non-reinforced section in design equations affects the safety factor. The code equations can lead to a less conservative design in lower grades of concrete and have a higher safety factor. However, the safety factor declines as compressive strength of concrete rises (higher variance of capacity of column section). The safety factor is more than 3 for reinforced and non-reinforced concrete and the structure possesses the essential safety in accordance with previous studies. Given the increased numerator of safety factor, it decreases as the range of compressive strength (compressive strength variance) of concrete increases.

7. Results and Discussion

In this study, the effect of concrete grade and reinforcement bar were investigated on the performance of CFT columns. The result of this study indicates that total displacement (U) increases with increment of concrete grade as well as capacity of column while the stress of CFT decreases. Figure 20 shows the rate of increment for all of samples which were obtained by using Equation 4.

$$\%\ rate\ = \frac{The\ maximum\ value\ for\ other\ smaples}{The\ maximum\ value\ for\ sample\ C20} \quad (4)$$

In Figure 20b and c, the blue bar graph represents the ratio of variables considered for reinforced columns (groups 2 and 3) to non-reinforced column C20 grade of concrete and the other loads indicate the ratio of C20, C30, C40 and C50 to the same group. The addition of reinforcement and enhancement of its percentage lead to an increase in the compressive and tensile capacity of section and also increases the Beta value. Figure 20b and c illustrate the increase in the 20 MPa grade of concrete. As shown in Figure 20b and c, the addition of reinforcement increases the BETA value in entire grades of concrete in comparison to the C20 grade of concrete. Figure 20b and c demonstrate that the addition of reinforcement to different grades of concrete causes maximum displacement of designed column to occur in the compression region, indicating an increase in the flexibility of column but no significant influence on the displacement of column in its compression region. According to the figure, increasing the grade of concrete up to C50 can enhance the compressive capacity of column by 3.15 times and its tensile capacity by 1.32 times, which are considerable values. Moreover, the increased grade of concrete reduces the safety of design equations with the maximum safety factor for the C20, C30, C40 and C50, respectively; so that the value rises as the reinforcement increases. Generally, the bigger area below the graph represents higher energy absorption and more ductile behavior of the structural element. In brick panels or specimen 1, concrete and brick layers tend to absorb most of the seismic load due to higher energy absorption by the system and crack initiation in concrete panels. As loading cycles increase, the rigidity of system decreases gradually, indicated by the slope of last cycles.

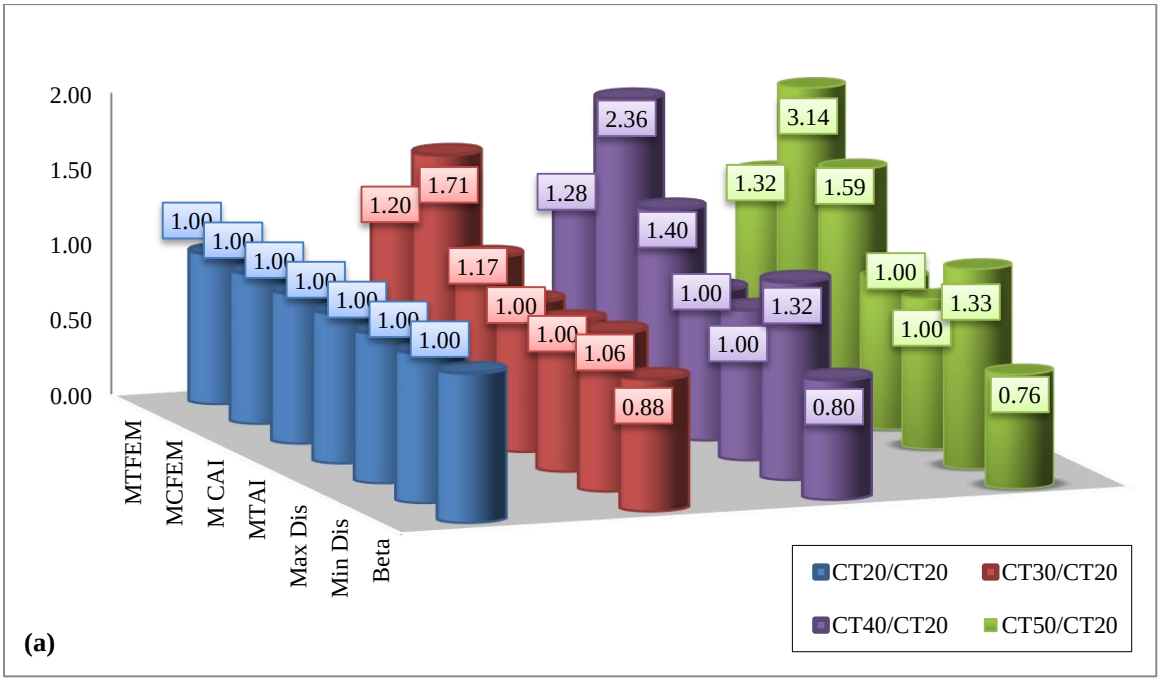

(a)

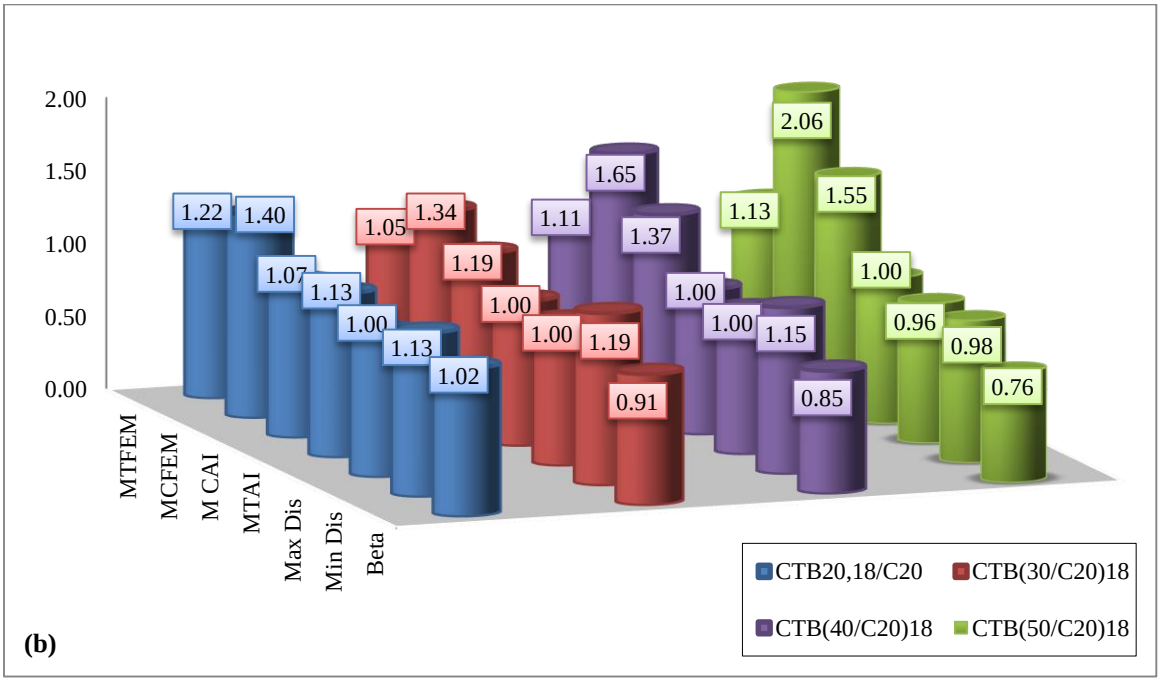

(b)

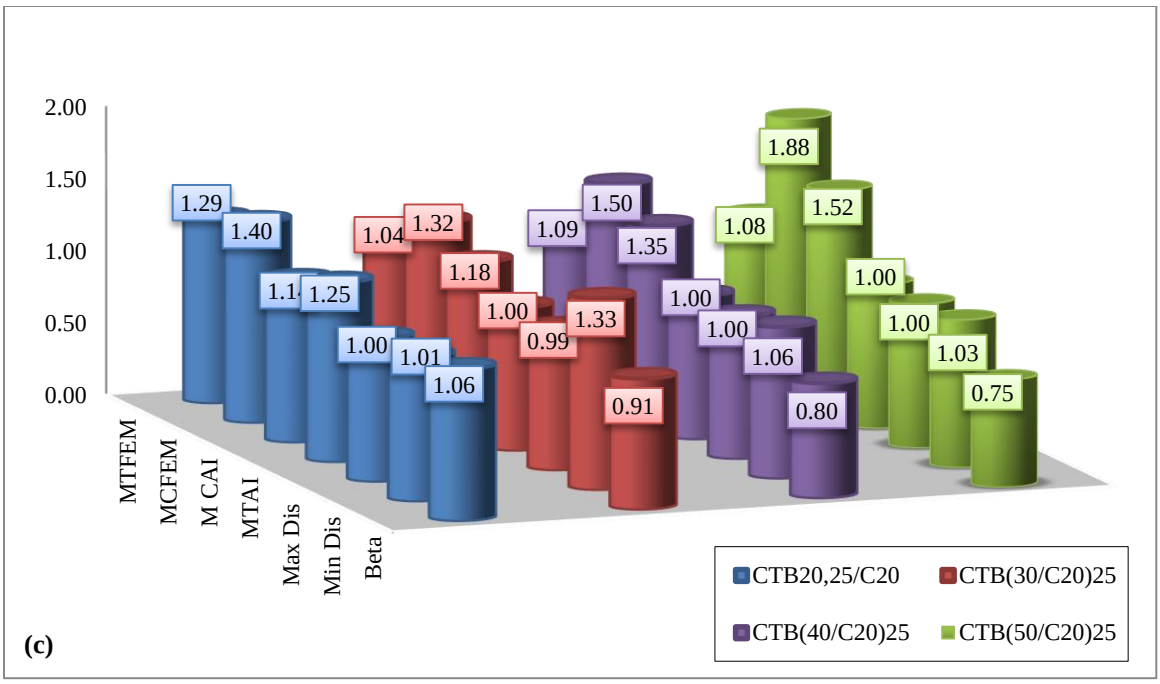

Figure 20. Fit toolbox results for the neural network result

By comparing the results from ABAQUS software and the suggested value of the regulation in the tensile region, the analytical value is found to be about 10% higher than the regulation values. In the compressive region, the analytical values linearly exceed the AISC values by increasing the compressive strength. It is suggested that in the design of CFT columns, the effect of column slenderness should be considered separately in the presented relations. In Figure 20, the increase in compressive strength of the CFT column was shown relative to various concrete strengths, which indicates an increase in the difference between the results of the analysis from the ABAQUS software and the values of the regulation with the increase in the compressive strength of concrete.

8. Conclusions

- According to the results obtained from the analysis in ABAQUS software, it was found that in tension, the steel section effectively resists the axial force, and in compression, the concrete mainly increases the buckling strength of the steel section by causing delay in the local buckling during the loading.
- In the relations presented in the AISC, the tensile strength of concrete is ignored in the tensile region, and the results of the analysis confirm the accuracy of the relations.
- In general, increasing the compressive strength of concrete in the tensile region did not affect the behavior of CFT column, but comparing the results of the software analysis with the values from the tenth chapter regulation indicates that the regulation relations are conservative, about 10%.
- Increasing the compressive strength of concrete in the compressive region is effective in the behavior of CFT column and significantly increases the bearing capacity. Comparing the AISC relations, by increasing the compressive strength, the difference between the analytical and the regulation values is linearly increased.
- It is suggested that the design relations of the regulation in the tensile and compressive regions to be separately presented for different slenderness values.

9. Conflicts of Interest

The authors declare no conflict of interest.

10. References

[1] Hassan, Maha M., Hazem M. Ramadan, Mohammed N. Abdel-Mooty, and Sherif A. Mourad. "Behavior of Concentrically Loaded CFT Braces Connections." Journal of Advanced Research 5, no. 2 (March 2014): 243–252. doi:10.1016/j.jare.2013.03.005.

[2] Wang, Yanlei, Guipeng Chen, Baolin Wan, Hao Lin, and Jin Zhang. "Behavior of Innovative Circular Ice Filled Steel Tubular Stub Columns Under Axial Compression." Construction and Building Materials 171 (May 2018): 680–689. doi:10.1016/j.conbuildmat.2018.03.208.

[3] Deng, Y., C.Y. Tuan, Q. Zhou, and Y. Xiao. "Flexural Strength Analysis of Non-Post-Tensioned and Post-Tensioned Concrete-Filled Circular Steel Tubes." Journal of Constructional Steel Research 67, no. 2 (February 2011): 192–202. doi:10.1016/j.jcsr.2010.08.005.

[4] Pan, Jianrong, Peng Wang, Yanjun Zheng, Zhan Wang, and Deming Liu. "An Analytical Study of Square CFT Columns in Bracing Connection Subjected to Axial Loading." Advances in Civil Engineering 2018 (November 25, 2018): 1–15. doi:10.1155/2018/8618937.

[5] Ellobody, Ehab, Ben Young, and Dennis Lam. "Behaviour of Normal and High Strength Concrete-Filled Compact Steel Tube Circular Stub Columns." Journal of Constructional Steel Research 62, no. 7 (July 2006): 706–715. doi:10.1016/j.jcsr.2005.11.002.

[6] Gupta, P.K., S.M. Sarda, and M.S. Kumar. "Experimental and Computational Study of Concrete Filled Steel Tubular Columns Under Axial Loads." Journal of Constructional Steel Research 63, no. 2 (February 2007): 182–193. doi:10.1016/j.jcsr.2006.04.004.

[7] Han, Lin-Hai, Zhong Tao, and Guo-Huang Yao. "Behaviour of Concrete-Filled Steel Tubular Members Subjected to Shear and Constant Axial Compression." Thin-Walled Structures 46, no. 7–9 (July 2008): 765–780. doi:10.1016/j.tws.2008.01.026.

[8] Kuranovas, Artiomas, Douglas Goode, Audronis Kazimieras Kvedaras, and Shantong Zhong. "Load-Bearing Capacity of Concrete-Filled Steel Columns." Journal of Civil Engineering and Management 15, no. 1 (March 31, 2009): 21–33. doi:10.3846/1392-3730.2009.15.21-33.

[9] Abedi, K., A. Nabati, H. Afshin, and A. Ferdousi. "Investigation into Behavior of CFT Circular Columns under Long-Term Axial and Cyclic Loadings." Asian Journal of Civil Engineering (BHRC) 16, no. 3 (2015): 322-346.

[10] Yadav, Raghabendra, Baochun Chen, Huihui Yuan, and Zhibin Lian. "Analytical Behavior of CFST Bridge Piers under Cyclic Loading." Procedia Engineering 173 (2017): 1731–1738. doi:10.1016/j.proeng.2016.12.208.

[11] Lu, Zhao-Hui, Yan-Gang Zhao, Zhi-Wu Yu, and Cheng Chen. "Reliability-Based Assessment of American and European Specifications for Square CFT Stub Columns." Steel and Composite Structures 19, no. 4 (October 25, 2015): 811–827. doi:10.12989/scs.2015.19.4.811.

[12] Naseri, Farzad, Faezeh Jafari, Ehsan Mohseni, Waiching Tang, Abdosattar Feizbakhsh, and Mohsen Khatibinia. "Experimental Observations and SVM-Based Prediction of Properties of Polypropylene Fibres Reinforced Self-Compacting Composites Incorporating Nano-CuO." Construction and Building Materials 143 (July 2017): 589–598. doi:10.1016/j.conbuildmat.2017.03.124.

[13] Khotbehsara, Mojdeh Mehrinejad, Bahareh Mehdizadeh Miyandehi, Farzad Naseri, Togay Ozbakkaloglu, Faezeh Jafari, and Ehsan Mohseni. "Effect of SnO 2 , ZrO 2 , and CaCO 3 Nanoparticles on Water Transport and Durability Properties of Self-Compacting Mortar Containing Fly Ash: Experimental Observations and ANFIS Predictions." Construction and Building Materials 158 (January 2018): 823–834. doi:10.1016/j.conbuildmat.2017.10.067.

[14] Ghanei, Amir, Faezeh Jafari, Mojdeh Mehrinejad Khotbehsara, Ehsan Mohseni, Waiching Tang, and Hongzhi Cui. "Effect of Nano-CuO on Engineering and Microstructure Properties of Fibre-Reinforced Mortars Incorporating Metakaolin: Experimental and Numerical Studies." Materials 10, no. 10 (October 23, 2017): 1215. doi:10.3390/ma10101215.

[15] Beheshti-Aval, S. B. "Strength evaluation of concrete-filled steel tubes subjected to axial-flexural loading by ACI and AISC-LRFD codes along with three dimensional nonlinear analysis." International Journal of Civil Engineering 10, no. 4 (2012): 280-290.

[16] Akbari, Jalal, Faeze Jafari, and Alireza Jahanpour. "Evaluation of Safety Index and Calibration of Load and Resistance Factors for Reinforced Concrete Beams under Bending, Shear and Torsion Demands." (2017): 49-64.

[17] Akbari, Jala, and Faezeh Jafari. "Calibration of Load and Resistance Factors for Reinforced Concrete." Civil Engineering Infrastructures Journal 51, no. 1 (2018): 217-227. doi:10.7508/CEIJ.2018.01.012.

[18] Guler, Soner, Erol Lale, and Metin Aydogan. "Behaviour of SFRC Filled Steel Tube Columns Under Axial Load." Volume 9 Number 1 (2013): 14–25. doi:10.18057/ijasc.2013.9.1.2.

[19] ACI Committee. Building code requirements for structural concrete (ACI 318-05) and commentary (ACI 318R-05). American Concrete Institute, (2005). doi:10.14359/12026.

[20] Hsu, L. S., and C.-T. T. Hsu. "Complete Stress — Strain Behaviour of High-Strength Concrete under Compression." Magazine of Concrete Research 46, no. 169 (December 1994): 301–312. doi:10.1680/macr.1994.46.169.301.

[21] ABAQUS Version 13 (General Purpose Finite Element Analysis Software documentation).